Using oxygen isotopes to quantitatively assess residual CO2 saturation during the CO2CRC Otway Stage 2B Extension residual saturation test

Using oxygen isotopes to quantitatively assess residual CO_2 saturation during the CO2CRC Otway Stage 2B Extension residual saturation test

Sascha Serno[a,*], Gareth Johnson[a], Tara C. LaForce[b,c], Jonathan Ennis-King[b,c], Ralf Haese[b,d], Chris Boreham[b,e], Lincoln Paterson[b,c], Barry M. Freifeld[b,f], Paul J. Cook[b,f], Dirk Kirste[b,g], R. Stuart Haszeldine[a], Stuart M.V. Gilfillan[a]

[a] School of GeoSciences, The University of Edinburgh, Grant Institute, The King's Buildings, James Hutton Road, Edinburgh EH9 3FE, United Kingdom

[b] CO2CRC Limited, The University of Melbourne, Carlton, VIC 3010, Australia

[c] CSIRO Energy, Private Bag 10, Clayton South, Victoria 3169, Australia

[d] School of Earth Sciences, The University of Melbourne, Carlton, Victoria 3010, Australia

[e] Geoscience Australia, GPO Box 378, Canberra 2601, Australia

[f] Lawrence Berkeley National Laboratory, Berkeley, California 94720, United States of America

[g] Department of Earth Sciences, Simon Fraser University, 8888 University Drive, Burnaby, British Columbia V5A 1S6, Canada

*** Corresponding author:** Sascha Serno
School of GeoSciences
The University of Edinburgh
Grant Institute, The King's Buildings
James Hutton Road
Edinburgh EH9 3FE
United Kingdom
Phone: +44 1316507010
Fax: +44 1316507340
Email: Sascha.Serno@ed.ac.uk

Abstract

Residual CO_2 trapping is a key mechanism of secure CO_2 storage, an essential component of the Carbon Capture and Storage technology. Estimating the amount of CO_2 that will be residually trapped in a saline aquifer formation remains a significant challenge. Here, we present the first oxygen isotope ratio ($\delta^{18}O$) measurements from a single-well experiment, the CO2CRC Otway 2B Extension, used to estimate levels of residual trapping of CO_2. Following the initiation of the drive to residual saturation in the reservoir, reservoir water $\delta^{18}O$ decreased, as predicted from the baseline isotope ratios of water and CO_2, over a time span of only a few days. The isotope shift in the near-wellbore reservoir water is the result of isotope equilibrium exchange between residual CO_2 and water. For the region further away from the well, the isotopic shift in the reservoir water can also be explained by isotopic exchange with mobile CO_2 from ahead of the region driven to residual, or continuous isotopic exchange between water and residual CO_2 during its back-production, complicating the interpretation of the change in reservoir water $\delta^{18}O$ in terms of residual saturation. A small isotopic distinction of the baseline water and CO_2 $\delta^{18}O$, together with issues encountered during the field experiment procedure, further prevents the estimation of residual CO_2 saturation levels from oxygen isotope changes without significant uncertainty. The similarity of oxygen isotope-based near-wellbore saturation levels and independent estimates based on pulsed neutron logging indicates the potential of using oxygen isotope as an effective inherent tracer for determining residual saturation on a field scale within a few days.

Keywords: residual saturation, oxygen isotopes, Otway, geochemical tracer, CO_2 storage

1. Introduction

Geological storage of CO_2 in rock formations, as part of Carbon Capture and Storage (CCS), is a promising means of directly lowering CO_2 emissions from fossil fuel combustion (Metz et al., 2005). CO_2 can be stored in the subsurface in three different ways over short timescales: (1) structural trapping, where gaseous or liquid CO_2 is trapped beneath an impermeable cap rock, (2) residual trapping, the immobilisation of CO_2 through trapping within individual and dead end spaces between rock grains, and (3) solubility trapping, where CO_2 is dissolved into the reservoir water that fills the pores between rock grains. Mineral trapping of CO_2 as a result of chemical reactions of the injected CO_2 with the host rock, forming new carbonate minerals within the pores, is a longer term storage mechanism, likely to play a role in siliciclastic formations several hundreds of years after initiation of CO_2 injection (e.g., Audigane et al., 2007; Sterpenich et al., 2009; Xu et al., 2003, 2004; Zhang et al., 2009).

For accurately modelling the long term fate of CO_2 in a commercial-scale CCS project, it is of value to develop an efficient plan to quantitatively assess the amount of structural, residual and solubility trapping at the reservoir scale through a short-term test undertaken in the vicinity of an injection well prior to large-scale injection. Such a test would reduce risk and uncertainty in estimating the storage capacity of a formation and would provide a commercial operator with greater reassurance of the viability of their proposed storage site. This is particularly true for residual trapping of CO_2 which can play a major role for CO_2 plume migration, immobilisation, storage security and reservoir management (Doughty and Pruess, 2004; Ennis-King and Paterson, 2002; Juanes et al., 2006; Krevor et al., 2015; Qi et al., 2009). Despite the important role of residual trapping of CO_2 in commercial-scale CCS projects, there is a current lack of cost-effective and reliable methodologies to estimate the degree of residual trapping on the reservoir scale (Mayer et al., 2015).

Stable isotopes may be highly suitable for assessing the movement and fate of injected CO_2 in the formation since they fingerprint the injected CO_2 rather than being a co-injected

compound like perfluorocarbon tracers, Kr or Xe (Mayer et al., 2013). There are few sources of available oxygen other than the reservoir water within CO_2 storage reservoirs (Johnson et al., 2011; Mayer et al., 2015). Any other reservoir oxygen that is available for water-rock reactions is typically in isotopic equilibrium with the reservoir fluid due to relatively fast reaction kinetics in the water-carbonate system (e.g., Mills and Urey, 1940; Vogel et al., 1970). During CO_2 injection, a new major source of oxygen is added to the system in the form of supercritical CO_2. Isotopic equilibrium exchange proceeds rapidly between oxygen in CO_2 and oxygen in water of various salinities (Kharaka et al., 2006; Lécuyer et al., 2009). In most natural environments the amount of oxygen in CO_2 is negligible compared to the amount of oxygen in water. Consequently, the oxygen isotope ratio ($\delta^{18}O$) of water remains essentially constant and $\delta^{18}O$ of CO_2 approaches that of the water plus the appropriate isotopic enrichment factor between water and CO_2 ($\varepsilon \approx 10^3 \ln\alpha_{CO_2\text{-}H_2O}$), depending on the reservoir temperature (Bottinga, 1968). At CO_2 injection sites, due to the large quantities of CO_2 injected, CO_2 becomes a major oxygen source, and both CO_2 and water will change their $\delta^{18}O$ due to isotopic equilibrium exchange reactions if the injected CO_2 is isotopically distinct with respect to the baseline reservoir water (Barth et al., 2015; Johnson and Mayer, 2011; Johnson et al., 2011; Kharaka et al., 2006; Mayer et al., 2015). This has also been observed in natural settings characterised by vast amounts of free-phase CO_2 in contact with water produced from CO_2-rich springs, for example in south east Spain (Céron and Pulido-Bosch, 1999; Céron et al., 1998) or in Bongwana, South Africa (Harris et al., 1997). The change in reservoir water $\delta^{18}O$ due to isotopic exchange with CO_2 under conditions typical for CO_2 injection sites can be related to the fraction of oxygen in the system sourced from CO_2 (Barth et al., 2015; Johnson and Mayer, 2011; Johnson et al., 2011; Kharaka et al., 2006), and the fraction of oxygen sourced from CO_2 can be successfully used to assess volumetric saturation of free-phase and dissolved CO_2 in the reservoir (Johnson et al., 2011; Li and Pang, 2015).

CO2CRC Limited (CO2CRC) developed and has operated the CO2CRC Otway Facility in the Otway Basin near Nirranda South, Victoria, Australia, since 2004 (Sharma et al., 2007).

106 The facility allows for trial injection in multiple storage types, including a saline formation that
107 currently uses a single-well configuration. This configuration is ideal for the development of an
108 effective reservoir characterisation test prior to commercial-scale CO_2 injection (Paterson et
109 al., 2011). In 2011, the first single-well injection test (using the CRC-2 injection well) was
110 undertaken at the Otway facility using 150 t of injected CO_2 to quantify reservoir-scale residual
111 trapping of CO_2 in a saline formation in the absence of an apparent structural closure
112 (CO2CRC Otway Stage 2B – henceforth referred to as Otway 2B; Paterson et al., 2011, 2013,
113 2014). The target reservoir for the experiment was within the Paaratte Formation, a saline
114 formation at 1075-1472 m TVDSS (true vertical depth below mean sea level), with the target
115 interval for the Otway 2B experiment at 1392-1399 m TVDSS. Deep saline formations are the
116 most likely candidates for geological CO_2 storage because of their huge potential capacity and
117 their locations close to major CO_2 sources (Holloway, 2001). The Paaratte Formation, while
118 only used for research purposes, is a saline formation analogous to those proposed for
119 commercial-scale CO_2 injection and storage. Two of the original measurements of residual
120 CO_2 saturation were acquired using noble gas (Xe and Kr) tracer injection and recovery data
121 (LaForce et al., 2014), and pulsed neutron logging of the CRC-2 injection well (Schlumberger
122 Residual Saturation Tool; Dance and Paterson, 2016; Paterson et al., 2013, 2014). The
123 second part of the recent COCRC Otway Stage 2B Extension project (henceforth referred to
124 as Otway 2B Extension) was a smaller-scale repeat of these two residual saturation tests
125 using improved methodologies.

126 Here we present oxygen ($\delta^{18}O$) and hydrogen isotope ($\delta^{2}H$) data from produced water
127 and formation water (U-tube) samples, and oxygen isotope data from CO_2 samples from the
128 Otway 2B Extension. For the first time we estimate levels of residual trapping of CO_2 based
129 on oxygen isotope data from a single-well test. We compare our results with measures from
130 independent techniques to estimate residual saturation.

131

2. CO2CRC Otway Stage 2B Extension Project

The Otway 2B Extension was conducted in October-December 2014 over a time span of 80 days. The target formation for the Otway 2B experiments, the Paaratte Formation, is a complex interbedded formation of medium to high permeability sandstones and thin carbonaceous mud-rich lithologies, deposited in multiple progradations of delta lobes during the Campanian (Bunch et al., 2012; Dance et al., 2012; Paterson et al., 2013). The target interval for the Otway 2B experiments at 1392-1399 m TVDSS is characterised by well-sorted texturally submature deltaic sandstone dominated by quartz and low clay and feldspar contents, overlain by a diagenetic carbonate seal (Kirste et al., 2014; Paterson et al., 2013, 2014). The sandstone is characterised by a porosity of ~28%, an average permeability of 2.2 Darcy and a fluid salinity of 800 mg/L (Bunch et al., 2012; Dance et al., 2012). The target reservoir is overlain by a cemented interval and a thick non-reservoir lithofacies interval with a high sealing capacity (Paterson et al., 2013, 2014). The CRC-2 well is equipped with a U-tube geochemical sampling system (Freifeld et al., 2005) and a set of four pressure and temperature gauges at the top and bottom of the target interval for the Otway 2B experiments.

The aims of the Otway 2B Extension were to study differences in reservoir water quality in response to the injection of CO_2-saturated water with and without trace amounts of gas impurities (Phase 1), and to characterise the residual trapping levels of CO_2 after injection of pure CO_2 into the formation (Phase 2). Our study primarily focuses on Phase 2. However, to study baseline conditions in the reservoir during the entire project, samples were taken during the initial production of 535.8 t of water from the target interval prior to Phase 1 and during the water injection for Phases 1.1 (days 11-12) and 1.2 (days 35-36), the two push-pull tests characterising Phase 1. Further, samples of produced water from Phases 1.1 (day 35) and 1.2 (days 62-63) were taken. Operational details of Phase 1 are presented in a separate study (Haese et al., in prep.).

158 Phase 2 started with the production of 75.1 t of water on days 63-64 (Table 1). On day
159 65, 67 t of previously produced water was injected for the 'water test', together with Kr, Xe and
160 methanol dissolved into the water during the injection (Phase 2.1). Water production with U-
161 tube and production water sampling to study the tracer behaviour at reservoir conditions
162 without CO_2 in the formation commenced immediately after the injection, producing 122.2 t of
163 water on days 65-67. A pulsed neutron log was run on day 68 to provide a baseline for the
164 near-wellbore conditions prior to the drive to residual saturation. This was followed by the
165 injection of 109.8 t of pure CO_2 on days 68-72 (Phase 2.2). Immediately following the CO_2
166 injection, another pulsed neutron log was run to measure the CO_2 response to test if the near-
167 well saturation was consistent with the predictions. On days 72-74, 323.7 t of previously
168 extracted water, saturated with 17.5 t of CO_2, was injected to drive the reservoir to residual
169 saturation (Phase 2.3). The injected water that drives the reservoir to residual saturation was
170 fully saturated with CO_2 to avoid dissolving the residually trapped CO_2. The near-well
171 saturation was tested using a final pulsed neutron log. On day 75, 67.2 t of previously produced
172 water, now saturated with 3.9 t of CO_2 and containing trace amounts of Kr, Xe and methanol,
173 was injected, followed by production of 128.5 t of water with U-tube and water sampling over
174 three days. This allowed measurement of the tracer partitioning between water and residually
175 trapped CO_2 in the reservoir during the 'residual saturation test' (Phase 2.4). Finally, the
176 excess water remaining in the surface tanks was re-injected for disposal on days 78-80.
177 Downhole temperatures and pressures were recorded through the entire duration of the
178 project. The injected gas for the Otway 2B Extension was a mix of industrial CO_2 captured at
179 the Callide Oxyfuel pilot capture plant in Queensland (Callide CO_2) and food grade CO_2 (99.9
180 %) from the Boggy Creek well in the vicinity of the Otway site (BOC CO_2).

181

182

183 ## 3. Materials and Methods

184 **3.1 Materials**

185 Water and gas samples were collected using the U-tube system (Freifeld et al., 2005).
186 This system provides the advantage of collecting reservoir water at in situ reservoir pressure
187 of ~140 bar, so that the dissolved gas does not exsolve during the ascent of the sample fluid
188 from the reservoir. At Otway, pressurised water samples were collected in 150 mL stainless
189 steel Swagelok cylinders with needle valves on each end. The cylinder was connected to
190 either a 1 L, 5 L or 10 L Restek™ multi-layer gas bag with a polypropylene combo valve,
191 depending on the amount of gas expected. The cylinder was depressurised under controlled
192 conditions for approximately one hour to collect all of the produced CO_2 and other gases in
193 the gas bag. Wet chemical analyses including pH, alkalinity, electrical conductivity and salinity
194 were conducted on the produced water samples in the purpose-built field laboratory. After
195 processing the water samples in the field laboratory, the depressurised fluids were filtered to
196 0.45 µm and ~8 mL of the filtered fluid transferred into a 10 mL pre-evacuated BD© plastic
197 vacutainer through the self-sealing lid of the vacutainer using a hypodermic needle for
198 subsequent isotope analysis.

199 Injection waters were sampled downstream of the oxygen scavenger (see Paterson et
200 al., 2011, for a detailed description and illustration of the CRC-2 process flow setup).
201 Production waters in addition to U-tube samples were sampled directly from the production
202 water line after the degassing tank. The injection and production water samples were filtered
203 to 0.45 µm and transferred to 60 mL Nalgene bottles with tight fitting caps, with zero
204 headspace on filling to prevent evaporation.

205 A sample of the pure CO_2 gas from the nearby Boggy Creek production well (BOC CO_2)
206 was collected for stable isotope analyses in a 1 L gas bag directly from the BOC tanker.
207 Duplicate samples of the Callide industrial CO_2 were collected for isotopic analyses by
208 depressurising a 150 mL stainless steel Swagelok cylinder containing liquid CO_2 filled directly
209 from the Callide tanker.

3.2 Methods

Water and CO_2 samples were analysed at the Stable Isotope Geochemistry Laboratory at the School of Earth Sciences of the University of Queensland, Australia. Water samples were analysed for oxygen isotopes after standard CO_2 equilibration (Epstein and Mayeda, 1953) and for hydrogen isotopes after online equilibration at 40 °C with Hokko coils, using an Isoprime Dual Inlet Isotope Ratio Mass Spectrometer (DI-IRMS) coupled to a Multiprep Bench for online analysis. Delta values in water samples are reported in ‰ deviation relative to VSMOW (Vienna Standard Mean Ocean Water) for both oxygen and hydrogen isotopes according to

$$\delta_{sample} = \left(\frac{R_{sample}}{R_{standard}} - 1\right) \times 1000 \quad (1)$$

where R represents the $^{18}O/^{16}O$ and $^{2}H/^{1}H$ ratios of samples and standards, respectively. Analytical uncertainties for water $\delta^{2}H$ and $\delta^{18}O$ are ±2 ‰ (1σ – one standard deviation) and ±0.1 ‰ (1σ), respectively. All laboratory standards were calibrated against IAEA (VSMOW, SLAP, GISP) and USGS (USGS45, USGS46) international water standards.

CO_2 samples were analysed using an Isoprime/Agilent Gas Chromatograph-combustion-Isotope Ratio Mass Spectrometer (GC-c-IRMS). All samples were analysed using a 20:1 split. The gas chromatograph (GC) (with a 50 m × 320 µm × 5 µm CP-PoraBOND Q column) was set to a flow of 1.2 mL/min with an oven temperature of 40 °C. The $\delta^{18}O$ values of the CO_2 gas (reported in ‰; $\delta^{18}O_{CO_2}$) were normalised to the VSMOW scale following a 2-point normalisation (Paul et al., 2007). NBS18 and NBS19 international reference standards were analysed to confirm calibration of the $\delta^{18}O$ scale. The analytical uncertainty for $\delta^{18}O$ in gas samples is ±0.2 ‰ (1σ).

234

235 # 4. Results

236 ## 4.1 Hydrogen isotopes in water samples

237 Values of δ^2H in water samples remain relatively constant throughout the entire Otway
238 2B Extension (Fig. 1). All samples bar one of the duplicate samples from the initial water
239 production prior to Phase 1.1 and the first water sample from the CO_2-saturated water injection
240 of Phase 1.1 fall within the 1σ range (±1.78 ‰) of the average of all samples from the entire
241 Otway 2B Extension (-30.19 ‰; excluding the duplicate sample with much higher values from
242 the initial water production). Four water samples were collected from the injection water during
243 Phase 1.1, and the average of the four (-33.58 ± 1.00 ‰) is marginally outside of the 1σ range
244 of the average from all samples. Values of reservoir water δ^2H throughout the Otway 2B
245 Extension are similar to baseline reservoir water values during the previous Otway 2B
246 experiment in 2011 (~-25 to -33 ‰; Kirste et al., 2014). The water δ^2H of samples collected
247 directly from the production line into bottles and samples from the U-tube during both the water
248 and residual saturation tests show an excellent correlation within their analytical uncertainties.

249

250 ## 4.2 Oxygen isotopes in water samples

251 For reservoir water $\delta^{18}O$, almost all samples prior to the three days of water production
252 for Phase 2.4 fall in the 1σ range (0.19 ‰) of the average of these bottle and U-tube samples
253 (-6.01 ‰) (Fig. 2). This baseline value is similar to the values for the first Otway 2B experiment
254 in 2011 of around -5 to -6 ‰ (Kirste et al., 2014). Only the two samples of injection water for
255 Phase 1.2 ($\delta^{18}O$ of ~-5.6 to -5.7 ‰) as well as two samples from the water production prior to
256 Phase 2.1 ($\delta^{18}O$ of ~-6.4 ‰) fall outside of the 1σ range. During the three days of water
257 production for Phase 2.4 (days 75-77), when water samples in contact with CO_2 in the
258 reservoir were collected, a decrease was observed in $\delta^{18}O$ ratios of reservoir water in both the

bottle and U-tube samples to the lowest values recorded throughout the experiment of -6.63 ± 0.10 ‰ and -6.46 ± 0.10 ‰, respectively. This indicates a shift away from stable baseline conditions without CO_2 prior to Phase 2.4 (Fig. 2 and 3). In particular, the $\delta^{18}O$ values of both the bottle and U-tube samples from the last day of water production are clearly lower compared to the baseline conditions, while $\delta^{2}H$ values remain constant throughout the entire project (Fig. 3).

In contrast to $\delta^{2}H$, there is an offset between $\delta^{18}O$ values in water samples from bottles and the U-tube for the water and residual saturation tests (Fig. 2). Bottle samples have consistently lower $\delta^{18}O$ values compared to the U-tube samples, although the offset is not constant from sample to sample.

5. Discussion

5.1 Baseline Stable Isotope Conditions and Small-Scale Baseline Changes Prior to CO_2 Injection

Concurrently increasing or decreasing final water $\delta^{18}O$ ($\delta^{18}O^{f}_{H_2O}$) and $\delta^{2}H$ values of reservoir water compared to baseline values can indicate admixture of different waters with variable isotopic compositions, while a change in $\delta^{18}O^{f}_{H_2O}$ without any change in $\delta^{2}H$ suggests water-CO_2 interaction in the reservoir when mineral dissolution can be excluded (e.g., D'Amore and Panichi, 1985; Johnson and Mayer, 2011; Johnson et al., 2011). Both $\delta^{18}O$ and $\delta^{2}H$ of reservoir water prior to CO_2 injection remained relatively stable during these "baseline" conditions, with $\delta^{2}H$ of reservoir water showing no change from the stable baseline conditions during the entire Otway 2B Extension (Fig. 1 and 2). This provides strong evidence for no major evaporation or water mixing processes at surface or in the reservoir. Further, both $\delta^{18}O$

283 and δ^2H show similar baseline conditions compared to the 2011 Otway 2B experiment,
284 indicating that any free-phase CO_2 potentially remaining in the reservoir near the well at the
285 end of the previous Otway 2B experiment dissolved and only negligibly changed the $\delta^{18}O$
286 signature of the reservoir water between the end of the first and initiation of the second Otway
287 2B experiment.

288 This is also supported by numerical simulations that have been run to investigate the
289 distribution of fluids in the reservoir at the start of the Otway Stage 2B Extension. Detailed
290 geological data were used to construct a near-well radial grid for the reservoir unit, and the
291 complete sequence of production and injection of fluids from 2011 onwards, including tracers,
292 was simulated using the TOUGH2 simulator with the EOS7G equation of state module, which
293 can model methane, CO_2 and tracers. The simulations were matched against the relevant field
294 data for pressure, temperature and produced concentrations in the 2011 Otway Stage 2B
295 experiment, so this gives some confidence that the model accurately represents the reservoir
296 behaviour during the 2011 test and beyond. The details of these simulations will be reported
297 elsewhere. By running the model forward from the end of 2011 data, the prediction was that
298 at the beginning of the 2014 experiment, the free-phase CO_2 had been dissolved from the
299 immediate vicinity of the well. Any remaining free-phase CO_2 was predicted to be confined to
300 a thin layer at the top of the reservoir unit, and away from the well.

301 We collected two U-tube samples in duplicate from the initial water production prior to
302 Phase 1.1, and one of these duplicate samples shows higher δ^2H values compared to the
303 other U-tube sample collected just prior (Fig. 1). The oxygen isotope composition of the
304 duplicates of both initial water production samples is very similar and within the range of all
305 water samples collected prior to CO_2 injection during Phase 2 (Fig. 2). Since these two
306 samples from the initial water production were stored over six months in a refrigerator in a
307 Falcon tube with around 20 % cap space prior to analysis, and since both samples were
308 collected consecutively and one of the samples shows δ^2H values in accordance with the other
309 collected samples during the project (Fig. 1), the higher δ^2H values of one of the initial water

310 production samples can potentially be explained by storage contamination influencing only
311 hydrogen isotopes.

312 Only four samples fall outside of the 1σ range of the average of all samples prior to the
313 production phase of the residual saturation test for $\delta^{18}O$: the two samples of injection water
314 for Phase 1.2 and two samples from the water production prior to the water test. The injection
315 water for Phase 1.2, derived from a different surface storage tank as the water injected during
316 Phase 1.1, shows both slightly higher $\delta^{18}O$ and $\delta^{2}H$ compared to the water injected into the
317 formation around one month earlier during Phase 1.1 (Fig. 1 and 2), potentially indicating
318 minor evaporation processes and/or oxygenation of water in the surface storage tanks (Haese
319 et al., in prep.). At the end of the water production prior to Phase 2.1, more water (212.3 t)
320 was produced than injected during Phases 1.1 and 1.2 (202.2 t). Therefore, it is possible that
321 the last few tons of the water produced was either older reservoir water from prior to the Otway
322 2B Extension or a mixture of this considerably older reservoir water with injected water from
323 Phase 1. This could explain the lower $\delta^{18}O$ of the waters produced on the day before Phase
324 2.1.

325 The stability of reservoir water $\delta^{18}O$ prior to Phase 2.4 provides evidence that, with the
326 exceptions noted above, $\delta^{18}O$ remained stable during baseline conditions when reservoir
327 water was not in contact with free-phase CO_2. During the three days of water production of
328 Phase 2.4, a decrease in $\delta^{18}O$ of water in contact with free-phase CO_2 in the reservoir
329 occurred, indicating a clear shift from the stable baseline conditions (Fig. 2 and 3). This change
330 in water $\delta^{18}O$ can be used in the following to estimate the fraction of CO_2 that is residually
331 trapped in the reservoir.

332

333 **5.2 Estimation of Residual CO_2 Saturation Based on Oxygen Isotope Values of**
334 **Reservoir Water**

The method used here to estimate residual CO_2 saturation based on changes in $\delta^{18}O$ of reservoir water in contact with free-phase CO_2 is described in detail in Johnson et al. (2011). If the majority of oxygen in the system is sourced from CO_2, as is the case near the injection well after Phase 2.3, $\delta^{18}O_{CO_2}$ will dominate the water-CO_2 system. The $\delta^{18}O$ ratio of reservoir water will start to change from the baseline water oxygen isotope value, $\delta^{18}O^{b}_{H_2O}$, towards an end-member scenario where the water has a final water value $\delta^{18}O^{f}_{H_2O}$ lower than that of the injected CO_2 by the isotopic enrichment factor (Johnson et al., 2011). In this case, the fraction of oxygen in the system sourced from CO_2, $X^{o}_{CO_2}$, can be estimated using

$$X^{o}_{CO_2} = \frac{\left(\delta^{18}O^{b}_{H_2O} - \delta^{18}O^{f}_{H_2O}\right)}{\left(\delta^{18}O^{b}_{H_2O} + \varepsilon - \delta^{18}O_{CO_2}\right)} \quad (2)$$

The isotopic enrichment factor ε between CO_2 and water is reported in ‰ and determined using the equation defined by Bottinga (1968)

$$\varepsilon = -0.0206 \times \left(\frac{10^6}{T^2}\right) + 17.9942 \times \left(\frac{10^3}{T}\right) - 19.97 \quad (3)$$

where T is the reservoir temperature in Kelvin. This equation is valid at atmospheric conditions as well as elevated temperatures and pressures relevant for CCS projects (Becker et al., 2015; Bottinga, 1968; Johnson et al., 2011).

The water-CO_2 system for oxygen in a reservoir can be described quantitatively in terms of the averaged reservoir CO_2 saturation for the region contacted by CO_2 and measured with the water sample (S_{CO_2}) using

$$S_{CO_2} = \frac{\left(BX^{o}_{CO_2} + CX^{o}_{CO_2} - B\right)}{\left(A - B - AX^{o}_{CO_2} + BX^{o}_{CO_2} + CX^{o}_{CO_2}\right)} \quad (4)$$

with A referring to moles of oxygen in 1 L of free-phase CO_2 at reservoir conditions, B to moles of oxygen dissolved in 1 L water from CO_2 at reservoir conditions, and C to moles of

356 oxygen in 1 L water at reservoir conditions (Johnson et al., 2011). During Phase 2.3, the
357 injection of CO_2 and water generally matched the target ratio during most of the water injection
358 for the drive to residual. However, late during the injection, there were periods of delivery of
359 added CO_2 below the target, potentially resulting in some dissolution of residually trapped CO_2
360 near the wellbore. Thus, in this experiment estimates of S_{CO_2} based on oxygen isotopes
361 provide flow-weighted averages of CO_2 saturation, and we expect that S_{CO_2} levels in the
362 reservoir are variable over distance from the borehole, with lower saturation estimates near
363 the wellbore.

364 Eq. (4) was first applied during the enhanced oil recovery (EOR) Pembina Cardium CO_2
365 monitoring project in Alberta, Canada, to estimate S_{CO_2} (Johnson et al., 2011), and the
366 robustness of this approach has been validated using laboratory (Barth et al., 2015; Johnson
367 and Mayer, 2011) and theoretical studies (Li and Pang, 2015). It has been further shown by
368 Johnson et al. (2011) that the method outlined above provides S_{CO_2} estimates from the Frio
369 experiment in east Texas (USA) similar to estimates from an approach that did not assume
370 established isotopic equilibrium between water and CO_2 and that uses volumetric ratios of
371 water and CO_2 determined from known changes in water and CO_2 $\delta^{18}O$ (Kharaka et al., 2006).
372 The method can only be applied if isotopic exchange with minerals in the reservoir can be
373 excluded. Injected CO_2 may form carbonic acid and liberate oxygen from the minerals in the
374 reservoir, e.g. through calcite dissolution (Gunter et al., 1993). Based on detailed analyses of
375 all major and minor cations and anions indicating fluid-mineral reactions, including Si, Al, Ca,
376 Mg, K and $HCO3^-$, in reservoir water samples collected during Phase 1 (Haese et al., in prep.),
377 silicate mineral dissolution can be ruled out. Very minor carbonate mineral (calcite and
378 siderite) dissolution was observed. However, the amount of oxygen liberated from carbonate
379 will be very small compared to the total oxygen from CO_2 and water. Sterpenich et al. (2009)
380 demonstrated that less than 1% by mass of an oolitic limestone dissolved due to interaction
381 with CO_2-saturated water under experimental conditions (150 bar, 80 °C) at water-rock ratios
382 40 times higher than those typical for reservoirs considered for CO_2 injection. Further, since

the target interval of the reservoir is characterised by deltaic sandstones dominated by quartz and low clay and feldspar contents (Kirste et al., 2014; Paterson et al., 2013, 2014), any contribution of oxygen from dissolution of carbonate minerals to the total oxygen inventory in the target interval is negligible. Therefore, we conclude that we can eliminate isotopic exchange with minerals as a contribution to oxygen isotope changes in the reservoir water during the Otway 2B Extension.

As mentioned above, we observe an offset between $\delta^{18}O$ values in water samples collected directly from the production line and U-tube samples during the water and residual saturation tests, with lower $\delta^{18}O$ values in bottle compared to U-tube samples, while no change can be observed in $\delta^{2}H$ (Fig. 1 and 2). The isotopic equilibrium between water and injected CO_2 is established before CO_2 exsolves (Johnson et al., 2011). Consequently, the U-tube fluid, which is the formation fluid depressurised at atmospheric pressure and therefore not in contact with the atmosphere or reservoir gas over longer time scales, provides our best estimate of $\delta^{18}O^{f}_{H_2O}$ in the reservoir at the time of sampling. Consequently, we use the U-tube sample values to estimate CO_2 saturation in the following.

5.3 Uncertainties in Water and CO_2 Source Mixing

5.3.1 Water Baselines and Production

For the approach to estimate residual CO_2 saturation outlined above to be robust, it is essential to have a reliable baseline $\delta^{18}O$ for reservoir water. A total of 390.9 t of CO_2-saturated water was injected during Phases 2.3 (323.7 t) and 2.4 (67.2 t) prior to producing 128.5 t of water in Phase 2.4 (days 75-77). Consequently, we expect that the water produced in Phase 2.4 was a mixture of the injection water of Phases 2.3 and 2.4. The 323.7 t of CO_2-saturated water injected during Phase 2.3 (days 72-74) had an average water $\delta^{18}O$ of -6.07 ± 0.07 ‰ and $\delta^{18}O_{CO_2}$ of +27.65 ± 0.12 ‰ for the co-injected CO_2, resulting in a $\delta^{18}O$ value for the fully

CO_2-saturated water of -6.18 ± 0.07 ‰ at wellbore conditions. On day 75, 67.2 t of CO_2-saturated water containing noble gas tracers were injected for Phase 2.4, with an average water $\delta^{18}O$ of -5.79 ± 0.07 ‰ and $\delta^{18}O_{CO_2}$ of +29.30 ± 0.20 ‰ for the co-injected CO_2, resulting in a $\delta^{18}O$ value for the fully CO_2-saturated water of -5.86 ± 0.07 ‰ at wellbore conditions.

The Phase 2.3 (first) injection of CO_2-saturated water thus has a slightly different oxygen isotope signature compared to the injection water for Phase 2.4, resulting in the necessity to account for mixing of these two water masses in the reservoir to provide a reliable baseline value for the estimation of residual saturation on each of the three days of water production. We used the data on co-injected methanol to estimate the mixing ratio of the two water masses during the water production stage. Methanol is a non-reactive tracer that can be applied to study mixing of water masses in a reservoir (e.g., Haese et al., 2013; Tomich et al., 1973). The methanol concentration of the injected water in Phase 2.4 was 330 ± 20 ppm based on duplicate samples from the injection line, and three U-tube samples collected during injection. Methanol was measured in nearly all U-tube samples collected during the water production stage of Phase 2.4. The injected water for Phase 2.3 was sourced from two different water storage tanks, with the last 111 t of the water sourced from the same tank used for the water injection and production during Phase 2.1 (Tank 3), and therefore containing methanol. The other 212 t of the injection were sourced from another tank (Tank 2) containing low levels of methanol (around 25 ppm by mass). Mass balance calculations suggest that the methanol concentration in Tank 3 should have been around 130 ppm at the start of Phase 2.3. Two U-tube samples taken after the Phase 2.3 injection gave an average methanol concentration in the reservoir of 87.5 ppm, suggesting that the injection concentration may have been slightly less than the mass balance calculation would suggest.

Fig. 4 shows the U-tube data for the concentration of methanol in the back-produced water in Phase 2.4, with the horizontal axis normalised as the produced volume relative to the injected volume (67.2 t). If there was no mixing between the two masses of injected water,

then one would expect this to be a step function, but there is obviously a degree of mixing, and this is determined by the hydrodynamic dispersion of the reservoir unit around the well.

A simple theoretical result can be obtained for the effect of longitudinal dispersion on the injection of a uniform tracer into a homogeneous reservoir with no initial tracer (Gelhar and Collins, 1971; Güven et al., 1985), and trivially modified for the case of a uniform background concentration of tracer already in the reservoir. Let C be the concentration of the tracer in the produced fluid, C_0 the injected tracer concentration, and C_b the uniform concentration of tracer already in the reservoir. Let x be the ratio of the cumulative volume of produced fluid at any time to the volume of the original injected fluid. The ratio of radial dispersivity α to the radial penetration depth of the tracer, R, is b. If the reservoir is perfectly stratified, and only longitudinal dispersion is considered, then

$$C=(C_0-C_b)\frac{1}{2}\ \mathrm{Erfc}\left(\frac{(x-1)}{\left(\frac{16\,b}{3}\left(2-|1-x|^{\frac{1}{2}}(1-x)\right)\right)^{1/2}}\right)+\ C_b \qquad (5)$$

In our case, it is only the last 111 t of water injected in Phase 2.3 that contain the tracer concentration C_b. After the injection of 67.2 t in Phase 2.4, the last part of the back-production of 128.5 t will probably not be producing water beyond that 111 t, so we can consider the tracer concentration in the reservoir to be uniform. If the theoretical result is fit to the methanol data by varying C_0, C_b and b then the curve in Fig. 4 is obtained. The fitted value of C_0 is 331 ppm (with a standard error of 7.2 ppm), which agrees well with the measured concentration of injected methanol. The fitted value of C_b is 98.6 ppm (with a standard error of 8.7 ppm), which is close to the measured concentration in the reservoir before the Phase 2.4 injection. The parameter b has a fitted value of 0.0177 (with a standard error of 0.0055). Numerical simulations indicate that the average radial penetration depth R of the tracer is about 3.5-3.8 m, so the fitted radial dispersivity α is 0.062 to 0.067 m.

457 The quality of the fit is worst during the early back-production, and this matches with
458 observations made in other similar continuous injection tracer tests (Güven et al., 1985).
459 Hydrodynamic dispersion acts to smooth out tracer concentrations, and since the tracer that
460 was first produced was that last injected (and which has been subject to the least dispersion),
461 this may explain some of the initial scatter in the tracer concentrations.

462 The theory can be extended to take account of permeability contrasts between layers,
463 but for the current test the corresponding result was barely different to the homogeneous case
464 with averaged properties, and so the calculations are not detailed here. Vertical dispersivity
465 has been ignored, although for larger injections into heterogeneous reservoirs this can cause
466 a much longer tail in the back-production, as the tracer disperses from the high permeability
467 layers into the low permeability ones.

468 The fitted analytical theory then gives a straightforward means of estimating the degree
469 of mixing in the reservoir, and the results are summarised in Table 2, where the range of the
470 prediction is obtained by varying the parameter b within the range of the standard error.

471

472 ***5.3.2 CO_2 Source***

473 A potential uncertainty in the estimation of residual CO_2 saturation using oxygen
474 isotopes can further result from the mixing of CO_2 from two different sources in the reservoir.
475 The first 12.2 t of the 109.8 t of pure CO_2 injected and residually trapped in the reservoir were
476 Callide CO_2 with a $\delta^{18}O$ ratio of +26.05 ± 0.14 ‰, while the remaining 97.6 t of pure CO_2 was
477 BOC CO_2 with an oxygen isotope signature of +29.30 ± 0.20 ‰. For the following estimation
478 of residual CO_2 saturation, we assumed perfect mixing of these two CO_2 sources in the
479 reservoir and derived the $\delta^{18}O_{CO_2}$ ratio to be used in Eq. (2) as a weighted average based on
480 the amounts of the two injected CO_2 sources. This results in a $\delta^{18}O_{CO_2}$ ratio for the residually
481 trapped CO_2 of +28.94 ± 0.12 ‰. We consider this approach as the most reliable to assess

482 $\delta^{18}O_{CO_2}$ since we do not have an estimate for the mixing of CO_2 in the reservoir or of variable
483 oxygen isotope signatures of CO_2 in contact with water in the reservoir.

484

485 **5.4 Estimates of Residual CO_2 Saturation in the Paaratte Formation**

486 For each U-tube sample collected for stable isotopes during the three days of water
487 production, we used Eqs. (2)-(4) to estimate residual trapping levels. We used the
488 thermodynamic model of Duan and Sun (2003) to derive solubilities and densities of CO_2 in
489 aqueous NaCl solutions under wellbore conditions for each individual day since temperatures
490 and pressures varied throughout the experiment (Table 3). As mentioned above, the average
491 wellbore temperatures and pressures for the times of U-tube sample collection were derived
492 from the four temperature and pressure gauges in the perforated interval

493 The first water production sample was collected ~7 hours after the start of water
494 production and ~9 hours after the end of CO_2-saturated water injection. With an isotopic
495 enrichment factor of 36.84 ‰ based on Eq. (3) and a $\delta^{18}O_{CO_2}$ value of +28.94 ± 0.12 ‰, we
496 expect the reservoir water in contact with free-phase CO_2 in the reservoir to change to lower
497 $\delta^{18}O$ values compared to the assumed $\delta^{18}O^{b}_{H_2O}$ value if isotopic equilibrium exchange
498 between reservoir water and CO_2 is established [Eq. (2)]. Our approach provides a value for
499 $X^{o}_{CO_2}$ of 0.13 ± 0.06 (Table 4). This indicates that enough oxygen sourced from CO_2 was
500 available in the reservoir to change the oxygen isotope signature of the reservoir water after
501 only a few hours. The $X^{o}_{CO_2}$ value provides a residual saturation estimate based on oxygen
502 isotopes of 14 ± 9 % [Eq. (4)].

503 For the second sample collected on day 76 with a $\delta^{18}O^{f}_{H_2O}$ value of -6.27 ± 0.10 ‰, the
504 methanol approach indicates that 22 ± 8 % of the oxygen in the water-CO_2 system is sourced
505 from the residually trapped CO_2, which results in a residual saturation estimate of 28 ± 11 %

(Table 4). The sample collected on the last day of Phase 2.4 (day 77) has the lowest $\delta^{18}O^{f}_{H_2O}$ value of all samples collected, with -6.46 ± 0.10 ‰, and is clearly distinct from the baseline water $\delta^{18}O$ prior to the injection of free-phase CO_2 (-6.01 ± 0.19 ‰) (Fig. 2 and 3). Our approach provides an $X^{o}_{CO_2}$ estimate of 32 ± 13 % (Table 4). This results in a residual saturation estimate in the target interval of 42 ± 16 %. Our data do not provide information about the timing of established final isotopic equilibrium between oxygen in water and CO_2 in the reservoir, with previous laboratory studies showing that final isotopic equilibrium at reservoir conditions normally encountered during CCS projects (up to 190 bar and 90 °C) is reached within a one-week period (Becker et al., 2015; Johnson and Mayer, 2011).

While our oxygen isotope data from reservoir water show a clear shift as a result of water-CO_2 isotopic exchange in the reservoir within a few days, our estimates of residual CO_2 saturation are characterised by relatively large uncertainties. Several factors can result in uncertainties in the oxygen isotope approach. First, and most importantly, the oxygen isotopic distinction between the injected CO_2 and baseline reservoir water in consideration of the isotopic enrichment factor at wellbore conditions is relatively small during the Otway 2B Extension. While a predictable $\delta^{18}O$ shift to lower values in reservoir water in contact with free-phase CO_2 compared to baseline conditions was observed, the small isotopic distinction of the two main oxygen sources resulted in a small isotopic shift in the short time of the Otway 2B Extension and a large uncertainty in S_{CO_2} estimates. Second, there are uncertainties resulting from the field experiment procedure and setup due to variable reservoir conditions during the entire project and uncertainty in the mixing ratios of water masses and CO_2 sources with different isotopic signatures. These uncertainties result in the necessity to make assumptions about mixing ratios of gases and water masses in the reservoir, and about average reservoir conditions during the different phases. The wellbore conditions during the Otway 2B Extension were slightly different compared to the reservoir conditions; in particular, injection temperatures were lower compared to reservoir temperatures (~59 °C; Bunch et al., 2012; Dance et al., 2012). Since it is uncertain at which exact temperature the isotopic

exchange reactions between free-phase CO_2 and brine occurred in the reservoir, the difference in injection versus reservoir temperature presents an uncertainty in the estimation of residual CO_2 saturation. All these factors can result in larger uncertainties than ideal in the baseline values of CO_2 and reservoir water, and the isotopic enrichment factors assumed for the reservoir.

5.5 Comparison of Independent Estimates of Residual CO_2 Saturation

We can compare our residual S_{CO_2} results from the three days of water production to independent estimates of residual CO_2 saturation in the Otway 2B target interval based on noble gas tracers and pulsed neutron logging from the first Otway 2B experiment. For the comparison of results from the two Otway 2B field experiments, we have to consider that differences in residual saturation levels between the two experiments can result from differences in the timing in events, especially during the water flood.

All three techniques to be compared measure a spatially varying residual saturation over different depths of investigation using different forms of averaging, and are characterised by specific uncertainties and limitations that have to be considered when comparing the results. Pulsed neutron logging provides residual CO_2 saturation levels in the vicinity of the well (~25 cm) at the point of time it is carried out (Adolph et al., 1994; Dance and Paterson, 2016). The CO_2 in the pulsed neutron logging may or may not be residually trapped, using the strict definition of a core test. Pulsed neutron logging and core flooding experiments have further provided evidence that there is a range of residual trapping values throughout a region contacted by CO_2, explained by the Land trapping model (Land, 1968). In this model, the final residual saturation is a function of the maximum CO_2 saturation, and the maximum CO_2 saturation varies throughout the region contacted by CO_2 (e.g., Dance and Paterson, 2016; Krevor et al., 2012, 2015; Land, 1968).

Tracer tests measure the CO_2 saturation achieved after the drive to residual, and provide a flow-weighted average of residual saturation on a larger reservoir scale compared to pulsed neutron logging, similar to oxygen isotopes. Therefore, the tracer data provide an estimate of residual CO_2 saturation for a larger reservoir rock volume characterised by residually trapped CO_2 and reservoir water (LaForce et al., 2014). The results based on numerical simulations of the noble gas data from the first Otway 2B experiment are potentially prone to uncertainties due to the consideration of a noble gas partitioning coefficients based on noble gas-water experiments at low pressures (Fernández-Prini et al., 2003), while recently new noble gas partitioning coefficients in a supercritical CO_2-water system at reservoir conditions became available and show differences to the previously published ones for low-pressure systems (e.g., Warr et al., 2015).

Given the discussed uncertainties and limitations of the techniques, we can now compare the estimates based on oxygen isotope changes in reservoir water with the independent reconstructions of residual CO_2 saturation. The stable isotope sample collected just 7 hours after the start of water production provides a near-wellbore estimate of residual trapping of CO_2, and can therefore be best compared to measures based on pulsed neutron logging. Saturation profiles from the first Otway 2B experiment from pulsed neutron logging show an average residual saturation of 20 %, with an overall range of 7 to 32 % (Dance and Paterson, 2016). While we have to consider the possibility that the water sampled just 7 hours into the water production phase may not have achieved full isotopic equilibrium with residual CO_2 in the reservoir, our estimate for this first stable isotope sample of 14 ± 9 % is similar with the saturation level reconstructed from pulsed neutron logging. The stable isotope sample from the second and third day can be best compared to the estimates based on noble gas injection and recovery. Reconstructed residual CO_2 saturation levels from the multiphase flow simulations of noble gas injection and recovery are between 11 and 20 % for the first Otway 2B experiment (LaForce et al., 2014). These estimates fall in the range of possible S_{CO_2} values based on stable isotopes from the second day (28 ± 11 %), but are lower than the results from

585 the last day of the Phase 2.4 water production stage (42 ± 16 %). This trend of increasing
586 S_{CO_2} with distance from the wellbore based on the oxygen isotope shift in the reservoir water
587 is different to the spatial residual trapping distribution in the reservoir from numerical reservoir
588 simulations, which predict decreasing gas saturation with distance from the well, with residuals
589 not exceeding 20 % further from the injection well.

590 Three potential mechanisms can explain the reconstructed change in oxygen isotopes
591 in the reservoir water during the three days of water production of Phase 2.4. The observed
592 trend can be the result of (1) a higher residual further away from the wellbore that is not
593 reconstructed using the noble gas injection and recovery method, (2) contact of the produced
594 water from the last day of Phase 2.4 with the region of mobile CO_2 ahead of the region driven
595 to residual, and/or (3) higher residual saturation levels reconstructed from oxygen isotopes in
596 waters longer in contact with residually trapped CO_2 in different regions of the reservoir. The
597 region that has been driven to residual does not extend very far into the reservoir and mobile
598 CO_2 from further out may have been pulled towards the well during production. Therefore,
599 mechanism (2) could explain the high S_{CO_2} value reconstructed from the water sampled during
600 the last day of Phase 2.4, but not the higher residual saturation estimate from the second day
601 compared to the first day of water production during Phase 2.4. Mechanism (3) considers
602 alteration of the isotopic values of reservoir water during the back-production that might
603 complicate the interpretation of the oxygen isotope changes in terms of residual saturation in
604 the reservoir. The oxygen isotope shift in the reservoir water away from baseline values may
605 be simply due to the variable CO_2 volumes the waters were in contact with in the reservoir,
606 with water samples characterised by a longer residence time in the supercritical CO_2-water
607 system from the beginning to end of the production phase. During the back-production of
608 Phase 2.4, the water may have continued exchanging oxygen with residual CO_2 with variable
609 isotopic signatures in the different regions of the reservoir, resulting in further perturbation of
610 $\delta^{18}O^{f}_{H_2O}$. Since residual CO_2 in the different regions of the reservoir may have already been
611 in contact with other waters and has variable oxygen isotope values compared to the initially

injected $\delta^{18}O_{CO_2}$ value, and since it is uncertain if there was enough time for continuous isotopic equilibrium exchange of reservoir water on its way to the well during back-production, it is difficult to resolve the potential contribution of mechanism (3) with confidence. Therefore, we cannot estimate the effect of this mechanism for the observed changes in oxygen isotopes of the reservoir water during the experiment.

Consequently, we are left with three potential mechanisms to explain the observed oxygen isotope shift in reservoir waters during the residual saturation test, particularly further away from the well. Future modelling and laboratory efforts to study the behaviour of oxygen isotopes in the Paaratte Formation at reservoir conditions, considering timing of injection and production events similar to Stage 2 of the Otway 2B Extension, would help to test our observation of variable residual trapping distribution in the reservoir, and could help further exploring the validity of mechanisms (2) or (3). Until then, all three potential reasons have to be considered in the interpretation of the oxygen isotope shift during the three days of water production, and the true nature of the residual saturation distribution further away from the well remains uncertain. However, mechanisms (2) and (3) are improbable to explain the observed oxygen isotope shift from baseline values for the first stable isotope sample collected shortly after the start of back-production. Therefore, this first water sample is the most reliable of the water production samples in terms of reconstructing residual trapping of CO_2 in the formation. Since the reconstructed residual saturation based on oxygen isotopes from this sample is similar to near-wellbore residual saturation values based on pulsed neutron logging, oxygen isotopes during the Otway 2B Extension show potential as an inherent tracer for residual saturation in a single-well experiment that should be further explored in future field and laboratory experiments.

6. Conclusions and Future Prospect

638 Field experiments at EOR sites in Texas (Frio experiment) and Alberta (Pembina
639 Cardium CO_2 monitoring project) provide evidence for the viability of using oxygen isotopes
640 measured in reservoir water and CO_2 to estimate S_{CO_2} over timescales longer than one week
641 (Johnson et al., 2011; Kharaka et al., 2006). This is a parameter that has been difficult to
642 assess using previous monitoring techniques but one which is crucial for determining the
643 efficiency of a CO_2 storage site. The application of oxygen isotopes has further been supported
644 by laboratory rock core experiments (Barth et al., 2015; Johnson and Mayer, 2011), water data
645 from CO_2-rich springs (e.g., Céron and Pulido-Bosch, 1999; Céron et al., 1998; Harris et al.,
646 1997), and theoretical studies (Li and Pang, 2015). Our study is the first to provide evidence
647 for a shift in oxygen isotope ratios of reservoir water due to isotopic equilibrium exchange with
648 free-phase CO_2 in a reservoir over only a few days, compared to stable baseline water values
649 prior to CO_2 injection (Fig. 2 and 3).

650 During Phase 2 of the Otway 2B Extension, the reservoir was characterised by residually
651 trapped CO_2 and fully CO_2-saturated reservoir water. In this setup, oxygen isotope changes in
652 the reservoir water can be used to estimate flow-weighted averages of residual CO_2
653 saturation. Our data provide residual trapping levels for reservoir rock volumes at different
654 distances from the wellbore. The other techniques used to study residual trapping during the
655 first Otway 2B experiment, noble gas tracers and pulsed neutron logging, are variable in their
656 spatial distribution of reconstructed trapping levels and have different depths of investigation
657 in the reservoir. The estimates of residual saturation based on oxygen isotopes from the
658 different days of water production indicate an increase in residual trapping levels with distance
659 from the wellbore. This trend of increasing residual saturation with distance from the wellbore
660 is not consistent with reservoir simulations, which predict the opposite trend. We show that
661 there are three potential mechanisms to explain the observed oxygen isotope shift from
662 baseline values for the water samples further away from the wellbore, resulting in considerable
663 uncertainty about the true residual saturation distribution in the reservoir at distance from the
664 well. However, only isotopic equilibrium exchange between water and residually trapped CO_2

665 can explain the isotopic shift in the water from near the wellbore. The similarity of the oxygen
666 isotope-based result from this water sample with independent estimates based on pulsed
667 neutron logging indicates that monitoring of oxygen isotope ratios of reservoir water in contact
668 with free-phase CO_2 may serve as an inexpensive inherent tracer with potential to reconstruct
669 flow-weighted averages for residual CO_2 saturation on a reservoir scale within a few days
670 without an additional tracer.

671 While our most reliable sample of reservoir water in contact with residually trapped CO_2
672 during the Otway 2B Extension indicates the potential of using oxygen isotopes to reconstruct
673 residual saturation in a single-well experiment, we show that the current setup of the Otway
674 2B Extension is not ideal to reconstruct residual trapping levels further away from the wellbore
675 using this tracer. Further, our residual trapping estimates based on oxygen isotopes are prone
676 to large uncertainties, which is mainly due to the small isotopic distinction of the baseline water
677 and CO_2 values leading to small predictable shifts in $\delta^{18}O$ of reservoir water in contact with
678 the injected CO_2. The setup of the field experiment, with two different sources of CO_2, injection
679 of two CO_2-saturated water masses with different oxygen isotope signatures, and lower
680 injection temperatures compared to reservoir temperatures, results in additional uncertainties
681 in the determination of baseline conditions and in the estimation of S_{CO_2}. For future
682 applications of this inherent tracer in an ideal single-well test, relatively simple measures can
683 be taken to reduce these uncertainties. It should be guaranteed that baseline reservoir water
684 and free-phase CO_2 are isotopically distinct enough to produce large shifts in the reservoir
685 water $\delta^{18}O$ as a result of water-CO_2 oxygen isotope exchange, resulting in small uncertainties
686 in S_{CO_2} estimates. This can be achieved by testing the isotopic signature of both oxygen
687 sources prior to the start of an experiment. In case of a small isotopic distinction, the CO_2 or
688 water to be injected may be isotopically spiked to further the distinction. The injection of CO_2
689 from a single source during the injection of pure CO_2 would increase the reliability and
690 precision of S_{CO_2} estimates. Injection temperatures similar to reservoir conditions further away

691 from the wellbore would further avoid uncertainties in the determination of the oxygen isotopic
692 enrichment factor in the reservoir, but this can be difficult to achieve in field operations.

693

694

695 ## Acknowledgements

696 This work was supported by funding from the UK CCS Research Centre (UKCCSRC)
697 through the Call 2 grant to S.M.V.G., G.J. and R.S.S., and the ECR International Travel
698 Exchange Fund to S.S. The UKCCSRC is funded by the EPSRC as part of the RCUK Energy
699 Programme. Funding for the Otway 2B Extension comes through CO2CRC, AGOS and
700 COSPL. The authors acknowledge the funding provided by the Australian government through
701 its CRC programme to support this CO2CRC research project. Funding for the group from the
702 Lawrence Berkeley National Laboratory was provided by the Carbon Storage Program, U.S.
703 DOE, Assistant Secretary for Fossil Energy, Office of Clean Coal and Carbon Management
704 through the NETL. We would like to thank Sue Golding and Kim Baublys for conducting stable
705 isotope measurements at the Stable Isotope Geochemistry Laboratory of the School of Earth
706 Sciences, University of Queensland, Australia. We appreciate the help in sample collection
707 from Jay Black, Hong Phuc Vu and the field operating team under the supervision of Rajindar
708 Singh. The paper was improved by constructive comments from two anonymous reviewers.

709

710

711 ## References

712 Adolph, B., Brady, J., Flaum, C., Melcher, C., Roscoe, B., Vittachi, A., Schnorr, D., 1994.
713 Saturation monitoring with the RST reservoir saturation tool. *Oilfield Rev.* 6, 29-39.

714 Audigane, P., Gaus, I., Czernichowski-Lauriol, I., Pruess, K., Xu, T.F., 2007. Two-
715 dimensional reactive transport modeling of CO_2 injection in a saline aquifer at the Sleipner
716 site, North Sea. *Am. J. Sci.* 307, 974-1008, doi:10.2475/07.2007.02.

717 Barth, J.A.C., Mader, M., Myrttinen, A., Becker, V., van Geldern, R., Mayer, B., 2015.
718 Avdances in stable isotope monitoring of CO_2 under elevated pressures, temperatures and
719 salinities: Selected results from the project CO_2ISO-LABEL, in: Liebscher, A., Münch, U.
720 (Eds.), Geological Storage of CO_2 - Long Term Security Aspects. Springer International
721 Publishing, Zürich, Switzerland, pp. 59-71.

722 Becker, V., Myrttinen, A., Nightingale, M., Shevalier, M., Rock, L., Mayer, B., Barth,
723 J.A.C., 2015. Stable carbon and oxygen isotope equilibrium fractionation of supercritical and
724 subcritical CO_2 with DIC and H_2O in saline reservoir fluids. *Int. J. Greenh. Gas Con.* 39, 215-
725 224, doi:10.1016/j.ijggc.2015.05.020.

726 Bottinga, Y., 1968. Calculation of fractionation fractors for carbon and oxygen isotopic
727 exchange in system calcite-carbon dioxide-water. *J. Phys. Chem.* 72, 800-808,
728 doi:10.1021/j100849a008.

729 Bunch, M.A., Daniel, R., Lawrence, M., Browne, G., Menacherry, S., Dance, T., Arnot,
730 M., 2012. Multi-scale characterisation of the Paaratte Formation, Otway Basin, for CO_2
731 injection and storage, in: Proceedings of the AAPG International Conference and Exhibition
732 2012, Singapore.

733 Céron, J.C., Pulido-Bosch, A., 1999. Geochemistry of thermomineral waters in the
734 overexploited Alto Guadalentín aquifer (South-East Spain). *Wat. Res.* 33, 295-300,
735 doi:10.1016/S0043-1354(98)00175-4.

736 Céron, J.C., Pulido-Bosch, A., de Galdeano, C.S., 1998. Isotopic idenfitication of CO_2
737 from a deep origin in thermomineral waters of southeastern Spain. *Chem. Geol.* 149, 251-258,
738 doi:10.1016/S0009-2541(98)00045-X.

739 D'Amore, F., Panichi, C., 1985. Geochemistry in geothermal-exploration. *Int. J. Energy*
740 *Res.* 9, 277-298, doi:10.1002/er.4440090307.

741 Dance, T., Paterson, L., 2016. Observations of carbon dioxide saturation distribution and
742 residual trapping using core analysis and repeat pulsed-neutron logging at the CO2CRC
743 Otway site. *Int. J. Greenh. Gas Con.* 47, 210-220, doi:10.1016/j.ijggc.2016.01.042.

744 Dance, T., Arnot, M., Bunch, M., Daniel, R., Ennis-King, J., Hortle, A., Lawrence, M.,
745 2012. Geocharacterisation and static modelling of the Lower Paaratte Formation: CO2CRC
746 Otway project stage 2, Technical Report RPT12-3481. CO2CRC, Canberra, Australia.

747 Doughty, C., Pruess, K., 2004. Modeling Supercritical Carbon Dioxide Injection in
748 Heterogeneous Porous Media. *Vadose Zone J.* 3, 837-847, doi:10.2136/vzj2004.0837.

749 Duan, Z.H., Sun, R., 2003. An improved model calculating CO_2 solubility in pure water
750 and aqueous NaCl solutions from 273 to 533 K and from 0 to 2000 bar. *Chem. Geol.* 193, 257-
751 271, doi:10.1016/S0009-2541(02)00263-2.

752 Ennis-King, J., Paterson, L., 2002. Engineering aspects of geological sequestration of
753 carbon dioxide, in: Proceedings of the SPE Asia-Pacific Oil and Gas Conference and
754 Exhibition 2002, Melbourne, Australia.

755 Epstein, S., Mayeda, T., 1953. Variation of O^{18} content of waters from natural sources.
756 *Geochim. Cosmochim. Ac.* 4, 213-224, doi:10.1016/0016-7037(53)90051-9.

757 Fernández-Prini, R., Alvarez, J.L., Harvey, A.H., 2003. Henry's constants and vapor
758 liquid distribution constants for gaseous solutes in H_2O and D_2O at high temperatures. *J. Phys.*
759 *Chem. Ref. Data* 32, 903-916, doi:10.1063/1.1564818.

760 Freifeld, B.M., Trautz, R.C., Kharaka, Y.K., Phelps, T.J., Myer, L.R., Hovorka, S.D.,
761 Collins, D.J., 2005. The U-tube: A novel system for acquiring borehole fluid samples from a

762 deep geologic CO_2 sequestration experiment. *J. Geophys. Res.* 110, B10203,
763 doi:10.1029/2005JB003735.

764 Gelhar, L.W., Collins, M.A., 1971. General analysis of longitudinal dispersion in
765 nonuniform flow. *Water Resour. Res.* 7, 1511-1521, doi:10.1029/WR007i006p01511.

766 Gunter, W.D., Perkins, E.H., McCann, T.J., 1993. Aquifer disposal of CO_2-rich gases:
767 Reaction design for added capacity. Energy Convers. Manage. 34, 941-948,
768 doi:10.1016/0196-8904(93)90040-H.

769 Güven, O., Falta, R.W., Molz, F.J., Melville, J.G., 1985. Analysis and interpretation of
770 single-well tracer tests in stratified aquifers. *Water Resour. Res.* 21, 676-684,
771 doi:10.1029/WR021i005p00676.

772 Haese, R.R., LaForce, T., Boreham, C., Ennis-King, J., Freifeld, B.M., Paterson, L.,
773 Schacht, U., 2013. Determining residual CO_2 saturation through a dissolution test – Results
774 from the CO2CRC Otway Project. *Energy Proc.* 37, 5379-5386,
775 doi:10.1016/j.egypro.2013.06.456.

776 Harris, C., Stock, W.D., Lanham, J., 1997. Stable isotope constraints on the origin of
777 CO2 gas exhalations at Bongwan, Natal. *S. Afr. J. Geol.* 100, 261-266,

778 Holloway, S., 2001 Storage of fossil fuel-derived carbon dioxide beneath the surface of
779 the earth. *Annu. Rev. Energy Env.* 26, 145-166, doi:10.1146/annurev.energy.26.1.145.

780 Hughes, C.E., Crawford, J., 2012. A new precipitation weighted method for determining
781 the meteoric water line for hydrological applications demonstrated using Australian and global
782 GNIP data. *J. Hydrol.* 464-465, 344-351, doi:10.1016/j.hydrol.2012.07.029.

783 Johnson, G., Mayer, B., 2011. Oxygen isotope exchange between H_2O and CO_2 at
784 elevated CO_2 pressures: Implications for monitoring of geological CO_2 storage. *Appl.*
785 *Geochem.* 26, 1184-1191, doi:10.1016/j.apgeochem.2011.04.007.

786 Johnson, G., Mayer, B., Nightingale, M., Shevalier, M., Hutcheon, I., 2011. Using oxygen
787 isotope ratios to quantitatively assess trapping mechanisms during CO_2 injection into
788 geological reservoirs: The Pembina case study. *Chem. Geol.* 283, 185-193,
789 doi:10.1016/j.chemgeo.2011.01.016.

790 Juanes, R., Spiteri, E.J., Orr, F.M., Jr., Blunt, M.J., 2006. Impact of relative permeability
791 hysteresis on geological CO_2 storage. *Water Resour. Res.* 42, W12418,
792 doi:10.1029/2005WR004806.

793 Kharaka, Y.K., Cole, D.R., Hovorka, S.D., Gunter, W.D., Knauss, K.G., Freifeld, B.M.,
794 2006. Gas-water-rock interactions in Frio Formation following CO_2 injection: Implications for
795 the storage of greenhouse gases in sedimentary basins. *Geology* 34, 577-580,
796 doi:10.1130/G22357.1.

797 Kirste, D., Haese, R., Boreham, C., Schacht, U., 2014. Evolution of formation water
798 chemistry and geochemical modelling of the CO2CRC Otway Site residual gas saturation test.
799 *Energy Proc.* 63, 2894-2902, doi:10.1016/j.egypro.2014.11.312.

800 Krevor, S.C.M., Pini, R., Zuo, L., Benson, S.M., 2012. Relative permeability and trapping
801 of CO_2 and water in sandstone rocks at reservoir conditions. *Water Resour. Res.* 48, W02532,
802 doi:10.1029/2011WR010859.

803 Krevor, S., Blunt, M.J., Benson, S.M., Pentland, C.H., Reynolds, C., Al-Menhali, A., Niu,
804 B., 2015. Capillary trapping for geologic carbon dioxide storage – From pore scale physics to
805 field scale implications. *Int. J. Greenh. Gas Con.* 40, 221-237, doi:10.1016/j.ijggc.2015.04.006.

806 LaForce, T., Freifeld, B.M., Ennis-King, J., Boreham, C., Paterson, L., 2014. Residual
807 CO_2 saturation estimate using noble gas tracers in a single-well field test: The CO2CRC Otway
808 project. *Int. J. Greenh. Gas Con.* 26, 9-21, doi:10.1016/j.ijggc.2014.04.009.

809 Land, C.S., 1968. Calculation of imbibition relative permeability for two- and three-phase
810 flow from rock properties. *SPE J.* 8, 149-156, doi:10.2118/1942-PA.

811 Lécuyer, C., Gardien, V., Rigaudier, T., Fourel, F., Martineau, F., Cros, A., 2009. Oxygen
812 isotope fractionation and equilibration kinetics between CO_2 and H_2O as a function of salinity
813 of aqueous solutions. *Chem. Geol.* 264, 122-126, doi:10.1016/j.chemgeo.2009.02.017.

814 Li, J., Pang, Z.H., 2015. Environmental isotopes in CO_2 geological sequestration.
815 *Greenh. Gas Sci. Technol.* 5, 1-15, doi:10.1002/ghg.1495.

816 Mayer, B., Shevalier, M., Nightingale, M., Kwon, J.-S., Johnson, G., Raistrick, M.,
817 Hutcheon, I., Perkins, E., 2013. Tracing the movement and the fate of injected CO_2 at the IEA
818 GHG Weyburn-Midale CO_2 Monitoring and Storage Project (Saskatchewan, Canada) using
819 carbon isotope ratios. *Int. J. Greenh. Gas Con.* 16S, S177-S184,
820 doi:10.1016/j.ijggc.2013.01.035.

821 Mayer, B., Humez, P., Becker, V., Dalkhaa, C., Rock, L., Myrttinen, A., Barth, J.A.C.,
822 2015. Assessing the usefulness of the isotopic composition of CO_2 for leakage monitoring at
823 CO_2 storage sites: A review. *Int. J. Greenh. Gas Con.* 37, 46-60,
824 doi:10.1016/j.ijggc.2015.02.021.

825 Metz, B., Davidson, O., de Coninck, H.C., Loos, M., Meyer, L.A., 2005. IPCC Special
826 Report on Carbon Dioxide Capture and Storage. Prepared by Working Group III of the
827 Intergovernmental Panel on Climate Change. Cambridge University Press, Cambridge, UK,
828 442 pp.

829 Mills, G.A., Urey, H.C., 1940. The kinetics of isotopic exchange between carbon dioxide,
830 bicarbonate ion, carbonate ion and water. *J. Am. Chem. Soc.* 62, 1019-1026,
831 doi:10.1021/ja01862a010.

832 Paterson, L., Boreham, C., Bunch, M., Ennis-King, J., Freifeld, B., Haese, R., Jenkins,
833 C., Raab, M., Singh, R., Stalker, L., 2011. The CO2CRC Otway stage 2B residual saturation
834 and dissolution test: test concept, implementation and data collected – Milestone report to
835 ANLEC 2011, CO2CRC Publication RPT11-3158. CO2CRC, Canberra, Australia.

836 Paterson, L., Boreham, C., Bunch, M., Dance, T., Ennis-King, J., Freifeld, B., Haese, R.,
837 Jenkins, C., LaForce, T., Raab, M., Singh, R., Stalker, L., Zhang, Y.Q., 2013. Overview of the
838 CO2CRC Otway residual saturation and dissolution test. *Energy Proc.* 37, 6140-6148,
839 doi.10.1016/j.egypro.2013.06.543.

840 Paterson, L., Boreham, C., Bunch, M., Dance, T., Ennis-King, J., Freifeld, B., Haese, R.,
841 Jenkins, C., Raab, M., Singh, R., Stalker, L., 2014. CO2CRC Otway Stage 2B residual
842 saturation and dissolution test, in: Cook, P.J. (Ed.), Geologically Storing Carbon: Learning
843 from the Otway Project Experience. CSIRO Publishing, Melbourne, Australia, pp. 343-380.

844 Paul, D., Skrzypek, G., Fórizs, I., 2007. Normalization of measured stable isotopic
845 compositions to isotope reference scales – a review. *Rapid Commun. Mass Spectrom.* 2,
846 3006-3014, doi:10.1002/rcm.3185.

847 Qi, R., LaForce, T.C., Blunt, M.J., 2009. Design of carbon dioxide storage in aquifers.
848 *Int. J. Greenh. Gas Con.* 3, 195-205, doi:10.1016/j.ijggc.2008.08.004.

849 Sharma, S., Cook, P., Berly, T., Anderson, C., 2007. Australia's first geosequestration
850 demonstration project - the CO2CRC Otway Basin Pilot Project. *APPEA J.* 47, 259-270.

851 Sterpenich, J., Sausse, J., Pironon, J., Géhin, A., Hubert, G., Perfetti, E., Grgic, D., 2009.
852 Experimental ageing of oolitic limestones under CO_2 storage conditons: Petrographical and
853 chemical evidence. *Chem. Geol.* 265, 99-112, doi:10.1016/j.chemgeo.2009.04.011.

854 Tomich, J.F., Dalton, R.L., Deans, H.A., Shallenberger, L.K., 1973. Single-well tracer
855 method to measure residual oil saturation. *J. Petrol. Technol.* 25, 211-218, doi:10.2118/3792-
856 PA.

857 Vogel, J.C., Grootes, P.M., Mook, W.G., 1970. Isotopic fractionation between gaseous
858 and dissolved carbon dioxide. *Z. Physik* 230, 225-238, doi:10.1007/BF01394688.

Warr, O., Rochelle, C.A., Masters, A., Ballentine, C.J., 2015. Determining noble gas partitioning within a CO_2-H_2O system at elevated temperatures and pressures. *Geochim. Cosmochim. Ac.* 159, 112-125, doi:10.1016/j.gca.2015.03.003.

Xu, T., Apps, J.A., Pruess, K., 2003. Reactive geochemical transport simulation to study mineral trapping for CO_2 disposal in deep arenaceous formations. *J. Geophys. Res.* 108, 2071, doi:10.1029/2002JB001979.

Xu, T., Apps, J.A., Pruess, K., 2004. Numerical simulation of CO_2 disposal by mineral trapping in deep aquifers. *Appl. Geochem.* 19, 917-936, doi:10.1016/j.apgeochem.2003.11.003.

Zhang, W., Li, Y., Xu, T., Cheng, H., Zheng, Y., Xiong, P., 2009. Long-term variations of CO_2 trapped in different mechanisms in deep saline formations: A case study of the Songliao Basin, China. *Int. J. Greenh. Gas Con.* 3, 161-180, doi:10.1016/j.ijggc.2008.07.007.

Figure captions

Figure 1: Water δ^2H from the Otway 2B Extension. Samples from injection periods (green (CO_2) and blue (water) bars at bottom of graph where numbers indicate tonnage) are shown as open symbols, while samples from production periods (orange bars, number = tonnage) are filled symbols. U-tube samples are shown as triangles, and bottle samples are squares. We differentiate by colour the initial water production and Phase 1.1 (black), Phase 1.2 (red), the early production phase in Phase 2 (magenta), Phase 2.1 (blue), and Phases 2.3 and 2.4 (green). Error bars show the analytical uncertainty of ±2 ‰. The black line indicates the average of all samples (excluding the duplicate sample with much higher values from the initial water production) ± 1σ uncertainty. Periods of pulsed neutron logging (red bars at bottom) are shown with production data.

Figure 2: Water $\delta^{18}O$ from the Otway 2B Extension. Samples from injection periods (green (CO_2) and blue (water) bars at bottom of graph where numbers indicate tonnage) are shown as open symbols, while samples from production periods (orange bars, number = tonnage) are filled symbols. U-tube samples are shown as triangles, and bottle samples are squares. We differentiate by colour the initial water production and Phase 1.1 (black), Phase 1.2 (red), the early production phase in Phase 2 (magenta), Phase 2.1 (blue), and Phases 2.3 and 2.4 (green). Error bars show the analytical uncertainty of ±0.1 ‰. The black line indicates the average of all samples from before the water production of the residual saturation test (prior to day 75) ± 1σ uncertainty. Periods of pulsed neutron logging (red bars at bottom) are shown with production data.

Figure 3: $\delta^{18}O$ vs. δ^2H in water samples from Phases 2.1, 2.3 and 2.4. Samples from injection and production periods are shown as open and filled symbols, respectively. U-tube samples are shown as triangles, and bottle samples as squares. Samples from Phase 2.1 are

907 in blue, from Phase 2.3 in red, from the water injection for Phase 2.4 in magenta, and for the
908 water production of Phase 2.4 in different green colours. The thick black line indicates the
909 local meteoric water line (LMWL) for Melbourne (Hughes and Crawford, 2012), and the black
910 box symbolises the 1σ range of the baseline water samples prior to water production for Phase
911 2.4.

912

913 **Figure 4**: Methanol concentration (ppm) in the back-produced formation water in Phase
914 2.4 (open circles), compared to the fit to a simple analytical theory described in the text (solid
915 line). The horizontal axis is the cumulative produced volume at a given time divided by the
916 total injected volume of 67.2 t.

917

918

919

920

921

922

923

924

925

926

927

928

Tables

Table 1: Time schedule of Phase 2 of the Otway 2B Extension. Days relate to the start of the Otway 2B Extension on 3 October 2014.

Day	Phase	Description	Injection CO_2 (t)	Injection Water (t)	Production Water (t)	Water rate (t/day)	CO_2 rate (t/day)
63-64		Water production			75.1	50.4	
65	2.1	Water injection with noble gases and methanol		67.0		199.5	
65-67	2.1	Water production			122.2	50.4	
68		Pulsed neutron logging					
68-72	2.2	Pure CO_2 injection	109.8				32.9
72		Pulsed neutron logging					
72-74	2.3	CO_2-saturated water injection	17.5	323.7		155.6	8.4
74		Pulsed neutron logging					
75	2.4	CO_2-saturated water injection with noble gases and methanol	3.9	67.2		155.1	9.0
75-77	2.4	Water production			128.5	49.5	

Table 2: Results of the methanol analysis for the fraction of the injected CO_2-saturated water mass for Phase 2.4 (second water mass) during the time intervals of U-tube sampling. The results are based on measured methanol concentrations in the U-tube samples and the fitted analytical model.

Day of experiment	Time	Produced water (t)	Fraction of production of second injected CO_2-saturated water mass
75	19:45 – 21:15	12.1	1.00
76	17:42 – 19:12	57.4	0.70 ± 0.13
77	19:20 – 20:50	110.2	0.04 ± 0.02

Table 3: Wellbore conditions for time periods of U-tube sampling during Phase 2.4. CO_2 solubilities and densities were estimated after Duan and Sun (2003). Parameters A, B and C are input parameters for Eq. (4).

Day	Time	Average temperature (°C)	Average pressure (bar)	CO_2 solubility (mol/kg)	CO_2 density (g/L)	A (mol/L) [Eq. (4)]	B (mol/L) [Eq. (4)]	C (mol/L) [Eq. (4)]
75	19:45 – 21:15	42.47	139.48	1.27	744.01	33.82	2.53	55.51
76	17:42 – 19:12	45.26	139.37	1.24	720.15	32.73	2.48	55.51
77	19:20 – 20:50	47.04	139.34	1.23	704.36	32.02	2.45	55.51

974 **Table 4**: Oxygen isotope-based results of residual CO_2 saturation using Eqs. (2)-(4) for the
975 three time intervals of U-tube sampling during Phase 2.4.

Day of experiment	Time	$\delta^{18}O^{b}_{H_2O}$ (‰ VSMOW)	ε [Eq. (3)] (‰)	$X^{o}_{CO_2}$ [1] [Eq. (2)]	S_{CO_2} [Eq. (4)]
75	19:45 – 21:15	-5.86 ± 0.07	36.84	0.13 ± 0.06	**0.14 ± 0.09**
76	17:42 – 19:12	-5.96 ± 0.05	36.34	0.22 ± 0.08	**0.28 ± 0.11**
77	19:20 – 20:50	-6.17 ± 0.07	36.03	0.32 ± 0.13	**0.42 ± 0.16**

976
977 [1] Calculated using a constant $\delta^{18}O_{CO_2}$ value of +28.94 ± 0.12 ‰ and measured $\delta^{18}O^{f}_{H_2O}$ values of -6.12 ± 0.10 ‰
978 for day 75, -6.27 ± 0.10 ‰ for day 76, and -6.46 ± 0.10 ‰ for day 77.

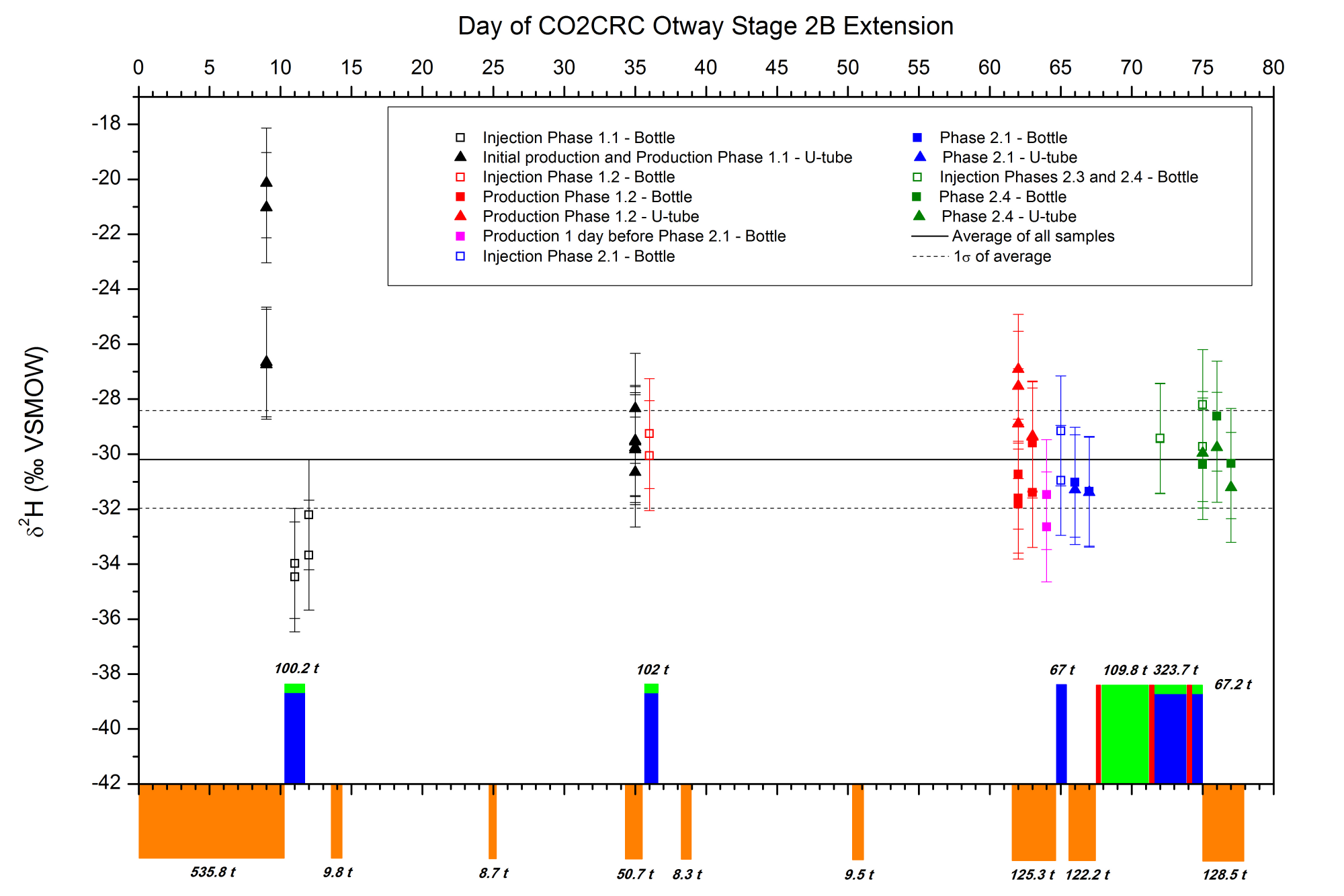
Day of CO2CRC Otway Stage 2B Extension
0
5
10
15
20
25
30
35
40
45
50
55
60
65
70
75
80
-18
-20
-22
-24
-26
-28
-30
-32
-34
-36
-38
-40
-42
δ2H (‰ VSMOW)
Injection Phase 1.1 - Bottle
Initial production and Production Phase 1.1 - U-tube
Injection Phase 1.2 - Bottle
Production Phase 1.2 - Bottle
Production Phase 1.2 - U-tube
Production 1 day before Phase 2.1 - Bottle
Injection Phase 2.1 - Bottle
Phase 2.1 - Bottle
Phase 2.1 - U-tube
Injection Phases 2.3 and 2.4 - Bottle
Phase 2.4 - Bottle
Phase 2.4 - U-tube
Average of all samples
1σ of average
100.2 t
102 t
67 t
109.8 t
323.7 t
67.2 t
535.8 t
9.8 t
8.7 t
50.7 t
8.3 t
9.5 t
125.3 t
122.2 t
128.5 t

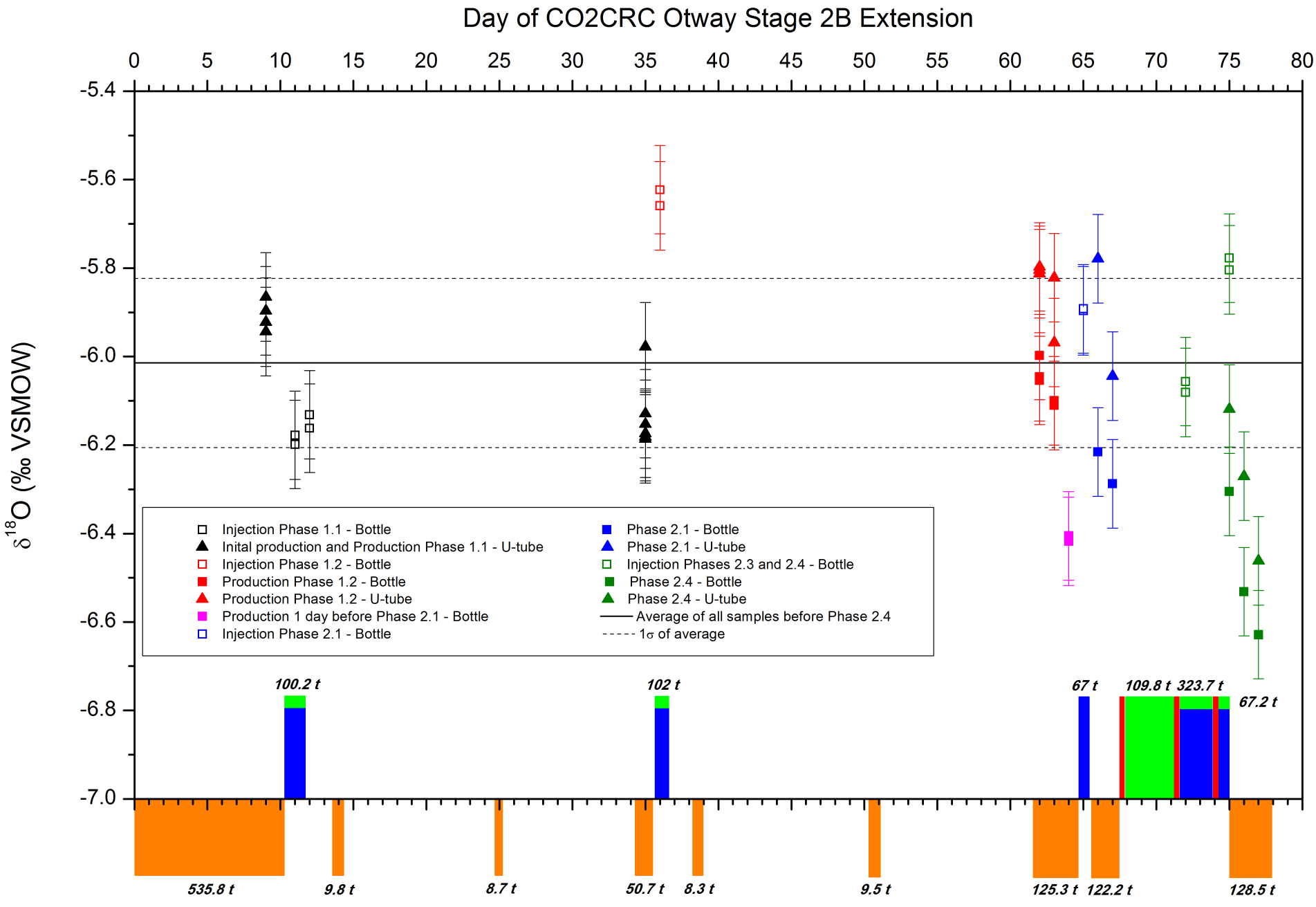
Day of CO2CRC Otway Stage 2B Extension
0
5
10
15
20
25
30
35
40
45
50
55
60
65
70
75
80
-5.4
-5.6
-5.8
-6.0
-6.2
-6.4
-6.6
-6.8
-7.0
δ18O (‰ VSMOW)
Injection Phase 1.1 - Bottle
Inital production and Production Phase 1.1 - U-tube
Injection Phase 1.2 - Bottle
Production Phase 1.2 - Bottle
Production Phase 1.2 - U-tube
Production 1 day before Phase 2.1 - Bottle
Injection Phase 2.1 - Bottle
Phase 2.1 - Bottle
Phase 2.1 - U-tube
Injection Phases 2.3 and 2.4 - Bottle
Phase 2.4 - Bottle
Phase 2.4 - U-tube
Average of all samples before Phase 2.4
1σ of average
100.2 t
102 t
67 t
109.8 t
323.7 t
67.2 t
535.8 t
9.8 t
8.7 t
50.7 t
8.3 t
9.5 t
125.3 t
122.2 t
128.5 t

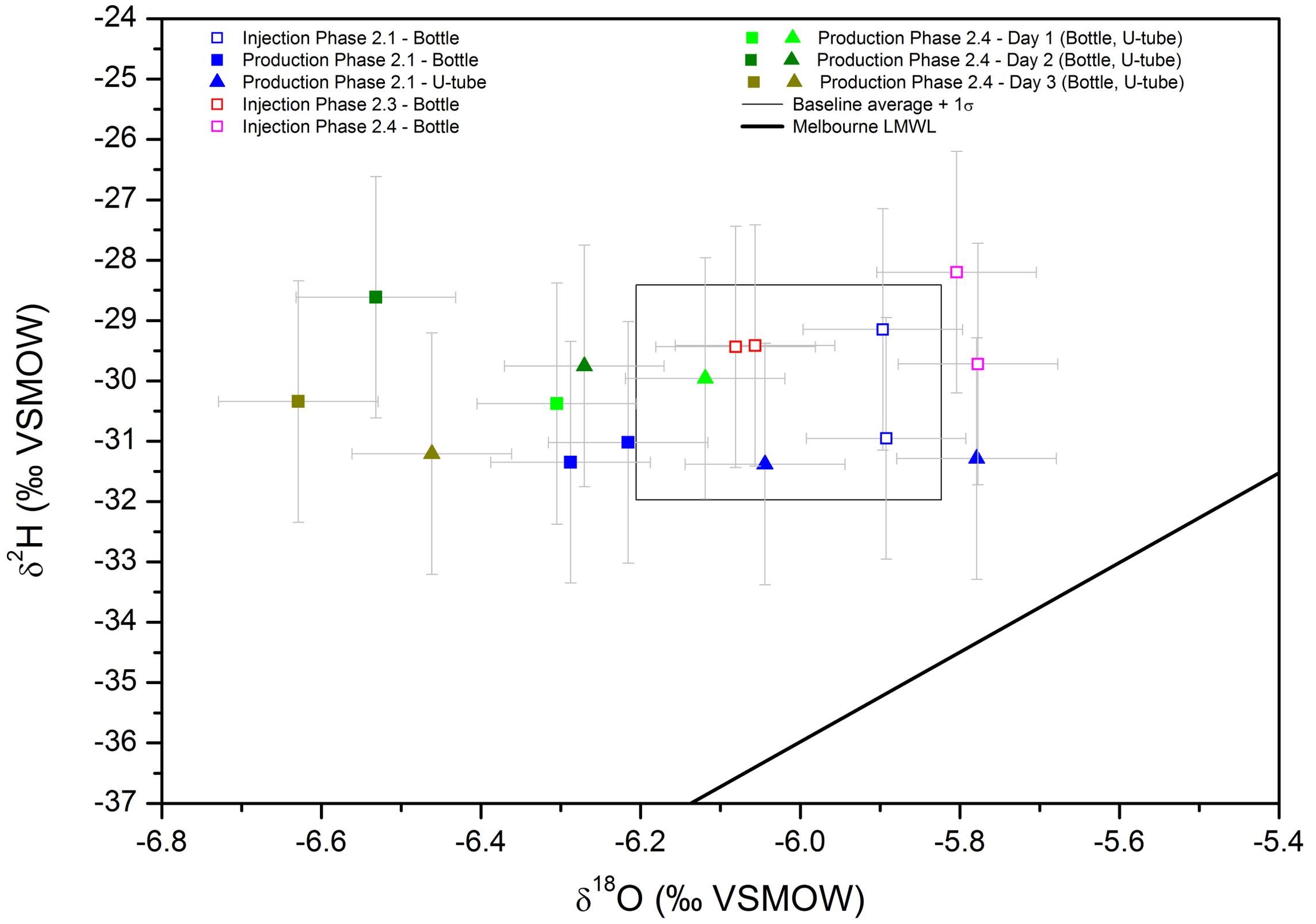
Injection Phase 2.1 - Bottle
Production Phase 2.1 - Bottle
Production Phase 2.1 - U-tube
Injection Phase 2.3 - Bottle
Injection Phase 2.4 - Bottle
Production Phase 2.4 - Day 1 (Bottle, U-tube)
Production Phase 2.4 - Day 2 (Bottle, U-tube)
Production Phase 2.4 - Day 3 (Bottle, U-tube)
Baseline average + 1σ
Melbourne LMWL
δ2H (‰ VSMOW)
δ18O (‰ VSMOW)
-24
-25
-26
-27
-28
-29
-30
-31
-32
-33
-34
-35
-36
-37
-6.8
-6.6
-6.4
-6.2
-6.0
-5.8
-5.6
-5.4

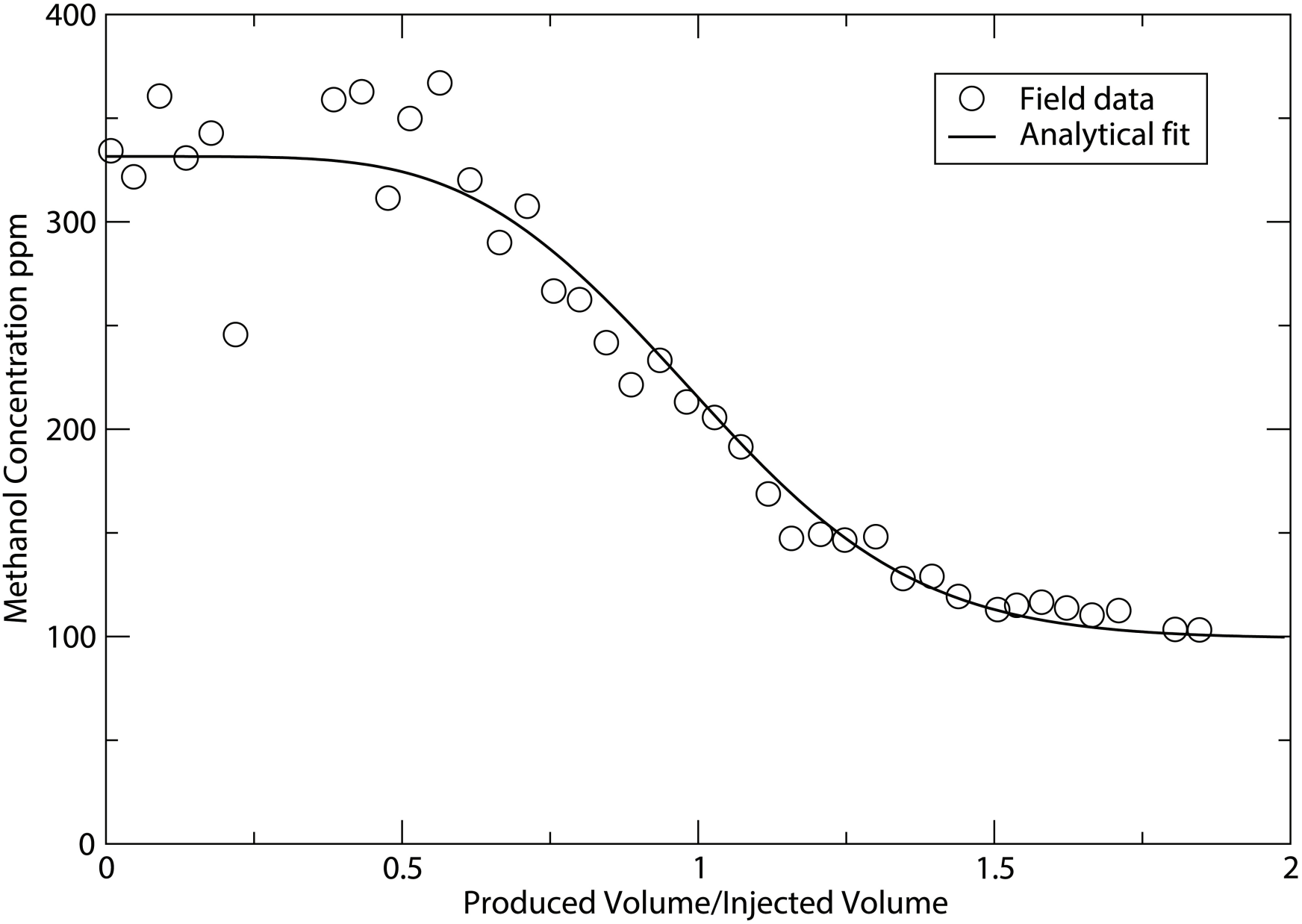
Field data
Analytical fit
Methanol Concentration ppm
Produced Volume/Injected Volume
0
100
200
300
400
0
0.5
1
1.5
2